Tad McGeer

School of Engineering Science
Simon Fraser University
Burnaby, British Columbia, Canada V5A 1S6

Passive Dynamic Walking

Abstract

There exists a class of two-legged machines for which walking is a natural dynamic mode. Once started on a shallow slope, a machine of this class will settle into a steady gait quite comparable to human walking, without active control or energy input. Interpretation and analysis of the physics are straightforward; the walking cycle, its stability, and its sensitivity to parameter variations are easily calculated. Experiments with a test machine verify that the passive walking effect can be readily exploited in practice. The dynamics are most clearly demonstrated by a machine powered only by gravity, but they can be combined easily with active energy input to produce efficient and dextrous walking over a broad range of terrain.

1. Static vs. Dynamic Walking

Research on legged locomotion is motivated partly by fundamental curiousity about its mechanics, and partly by the practical utility of machines capable of traversing uneven surfaces. Increasing general interest in robotics over recent years has coincided with the appearance of a wide variety of legged machines. A brief classification will indicate where our own work fits in. First one should distinguish between *static* and *dynamic* machines. The former maintain static equilibrium throughout their motion. This requires at least four legs and, more commonly, six. It also imposes a speed restriction, since cyclic accelerations must be limited in order to minimize inertial effects. Outstanding examples of static walkers are the Odex series (Russell 1983) and the Adaptive Suspension Vehicle (Waldron 1986). Dynamic machines, on the other hand, are more like people; they can have fewer legs than static machines, and are potentially faster.
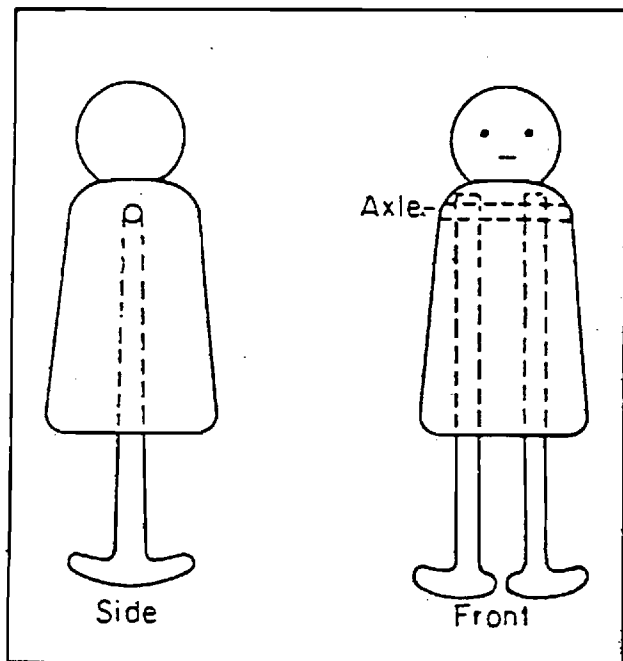
2. Dynamics vs. Control

Our interest is in dynamic walking machines, which for our purposes can be classified according to the role of active control in generating the gait. At one end of the spectrum is the biped of Mita et al. (1984), whose motion is generated entirely by linear feedback control. At the end of one step, joint angles are commanded corresponding to the end of the next step, and the controller attempts to null the errors. There is no explicit specification of the trajectory between these end conditions. Yamada, Furusho, and Sano (1985) took an approach that also relies on feedback, but in their machine it is used to track a fully specified trajectory rather than just to close the gap between start and end positions. Meanwhile the stance leg is left free to rotate as an inverted pendulum, which, as we shall discuss, is a key element of passive walking. Similar techniques are used in biped walkers by Takanishi et al. (1985), Lee and Liao (1988), and Zheng, Shen, and Sias (1988).

By contrast the bipeds of Miura and Shimoyama (1984) generate their gait by feedforward rather than feedback; joint torque schedules are precalculated and played back on command. Again the stance leg is left free. However, the "feedforward" gait is unstable, so small feedback corrections are added to maintain the walking cycle. Most significantly, these are *not* applied continuously (i.e., for tracking of the nominal trajectory). Instead the "feedforward" step is treated as a processor whose output (the end-of-step state) varies with the input (the start-of-step state). Thus the feedback controller responds to an error in tracking by modifying initial conditions for subsequent steps, and so over several steps the error is eliminated. In this paper you will see analysis of a similar process. Raibert (1986) has developed comparable concepts but with a more pure implementation, and applied them with great success to running machines having from one to four legs.

All of these machines use active control in some form to generate the locomotion pattern. They can be

Fig. 1. A bipedal toy that walks passively down shallow inclines. [Reprinted from (McMahon 1984).]

Fig. 2. General arrangement of a 2D biped. It includes legs of arbitrary mass and inertia, semicircular feet, and a point mass at the hip.

Axle

Side

Front

$-\Delta\theta_F$ $\Delta\theta_C$

m_H

m_C, r_{gyr_C}
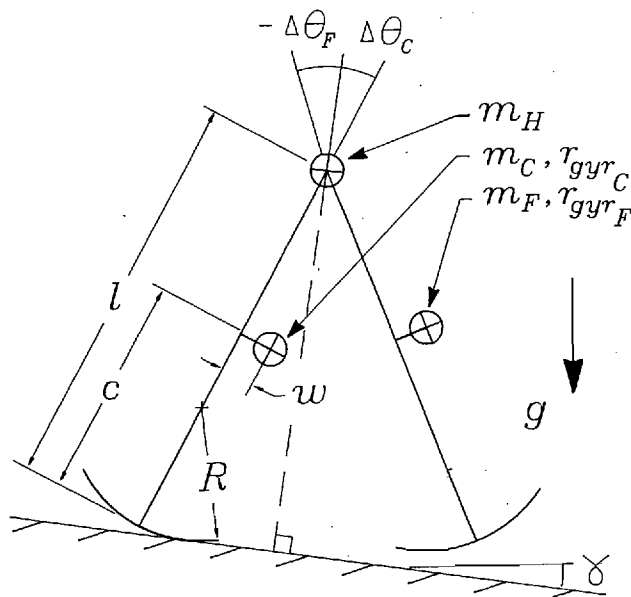
m_F, r_{gyr_F}

l

c

w

g

R

γ

ordered according to the style of implementation, ranging from continuous active feedback to once-per-step adjustment of an actively generated but nevertheless fixed cycle. This paper discusses a machine at the extreme end of the spectrum: gravity and inertia alone generate the locomotion pattern, which we therefore call "passive walking."

3. Motivation for Passive Walking

The practical motivation for studying passive walking is, first, that it makes for mechanical simplicity and relatively high efficiency. (The specific resistance of our test biped is ≈ 0.025 in a human-like walk.) Second, control of speed and direction is simplified when one doesn't have to worry about the details of generating a substrate motion. Moreover, the simplicity promotes understanding. Consider an analogy with the development of powered flight. The Wrights put their initial efforts into studying gliders, as did their predecessors Cayley and Lilienthal. Once they had a reason-

able grasp of aerodynamics and control, adding a powerplant was only a small change. (In fact, their engine wasn't very good even for its day, but their other strengths ensured their success.) Adding power to a passive walker involves a comparably minor modification (McGeer 1988).

Actually passive walkers existed long before contemporary research machines. My interest was stimulated by the bipedal toy shown in Figure 1; it walks all by itself down shallow slopes, while rocking sideways to lift its swing foot clear of the ground. A similar quadruped toy walks on level ground while being pulled by a dangling weight. I learned of such toys through a paper by Mochon and McMahon (1980), who showed how walking could be generated, at least in large measure, by passive interaction of gravity and inertia. Their "ballistic walking" model is especially helpful for understanding knee flexion, which is discussed toward the end of the paper.

Our discussion here is based on the model shown in Figure 2, which is no more than two stiff legs pinjointed at the hip. It can be regarded as a two-dimensional version of the toy; its dynamics in the longitudinal plane are similar, but it doesn't rock sideways. This simplifies the motion, but it left us with new problems in building a test machine: how to keep the
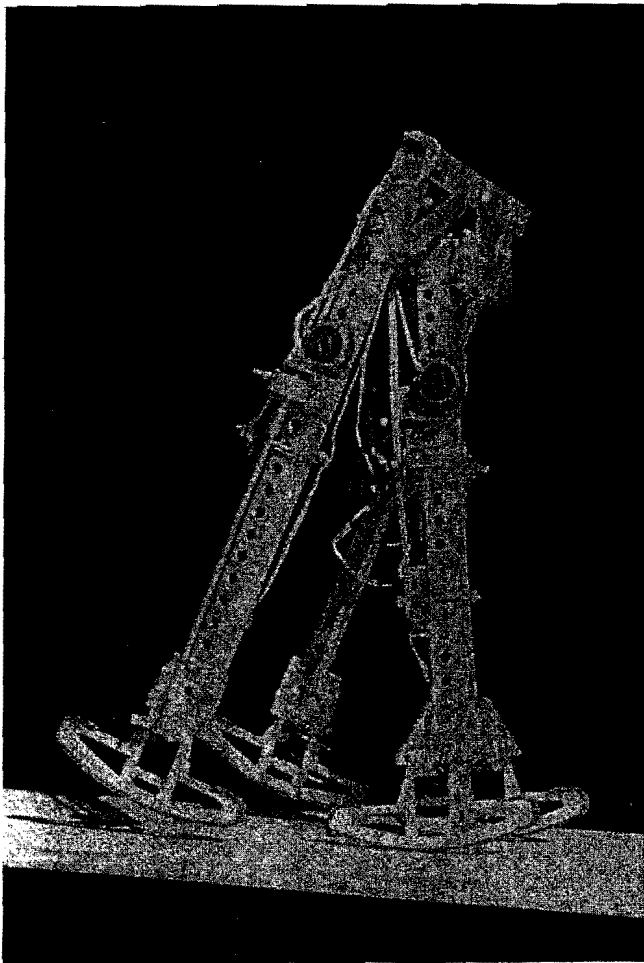
motion two-dimensional, and how to clear the swing foot. Figure 3 is a photo of our solution. Two-dimensionality is enforced by building the outer leg as a pair of crutches. Foot clearance is by either of two methods. Occasionally we use a checkerboard pattern of tiles, which in effect retract the ground beneath the swing feet. However, usually it is more convenient to shorten the legs; thus the machine can lift its feet via small motors driving leadscrews.

The discussion here begins with two elementary models to illustrate the energetics and dynamics of passive walking. Next follow analyses of cyclic walking and stability for the general model of Figure 2, and comparison with experimental results. Then comes a

survey of parametric effects, and finally some comments on extensions of the model.

4. Reinventing the Wheel

Imagine an ideal wagon wheel that can roll smoothly and steadily along a level surface, maintaining any speed without loss of energy. Its rolling seems quite different from walking (and on the whole more sensible!), but in fact rolling can be transformed to walking by a simple metamorphosis.

4.1. The Rimless Wheel

Following Margaria (1976), remove the rim from the wagon wheel as in Figure 4, leaving, in effect, a set of legs. Unlike the original wheel, this device cannot roll steadily on a level surface; instead it loses some speed each time a new leg hits the ground. We treat each of these collisions as inelastic and impulsive. In that case the wheel conserves angular momentum about the impact point, and the loss in speed can be calculated as follows. Immediately before the collision the angular momentum is

$$H^- = (\cos 2\alpha_0 + r_{gyr}^2)\, ml^2\Omega^-. \qquad (1)$$

(Note that the wheel's radius of gyration is normalized by leg length l.) Immediately after the collision, the angular momentum is simply

$$H^+ = (1 + r_{gyr}^2)\, ml^2\Omega^+. \qquad (2)$$

Equating these implies that

$$\frac{\Omega^+}{\Omega^-} = \frac{\cos 2\alpha_0 + r_{gyr}^2}{1 + r_{gyr}^2} = \eta. \qquad (3)$$

All of our analysis is cast in dimensionless terms, with mass m, leg length l, and time $\sqrt{l/g}$ providing the base

units. To define what amounts to a dimensionless pendulum frequency (7),

$$\sigma^2 \equiv \frac{1}{1 + r_{gyr}^2}.$$ (4)

Then

$$\eta = 1 - \sigma^2(1 - \cos 2\alpha_0).$$ (5)

It follows from (3) that over a series of k steps

$$\Omega_k \sim \eta^k.$$ (6)

Hence on a level surface the rimless wheel will decelerate exponentially. However, on a downhill grade, say with slope γ, the wheel can recoup its losses and so establish a steady rolling cycle. The equilibrium speed can be calculated from the differential equation for rotation about the stance foot. Over the range of angles used in walking, linearization for small angles is entirely justified, so the equation can be written as

$$\ddot{\theta} - \sigma^2\theta \approx \sigma^2\gamma.$$ (7)

Here θ is measured from the surface normal; thus the wheel has an unstable equilibrium at $\theta = -\gamma$.

One "step" begins with $\theta = -\alpha_0$, and rolling is cyclic if the initial speed, say Ω_0, repeats from one step to the next. Repetition of Ω_0 implies that each step must end with rotational speed Ω_0/η (6). Thus the steady step has the following initial and final states:

$$\begin{aligned} \theta(0) &= -\alpha_0 & \Omega(0) &= \Omega_0 \\ \theta(\tau_0) &= \alpha_0 & \Omega(\tau_0) &= \Omega_0/\eta \end{aligned}$$ (8)
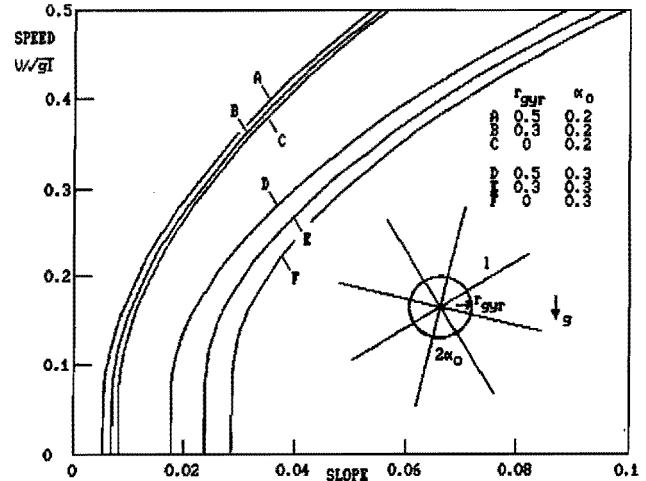
Both Ω_0 and the steady step period τ_0 can be evaluated by applying these boundary conditions to the equation of motion (7). The results are

$$\Omega_0 = \sqrt{\frac{4\gamma\alpha_0\sigma^2\eta^2}{1 - \eta^2}},$$ (9)

$$e^{\sigma\tau_0} = \frac{\gamma + \alpha_0 + \Omega_0/\sigma\eta}{\gamma - \alpha_0 + \Omega_0/\sigma}.$$ (10)

For small α_0 the dimensionless *forward* speed is then

$$V \approx \frac{2\alpha_0}{\tau_0}.$$ (11)

Figure 4 includes plots of this speed as a function of slope for various rimless wheels. These may be compared with speed versus slope in passive walking of a biped, which is plotted in Figure 6. The plots are qualitatively similar and quantitatively comparable. As an example, take $\alpha_0 = 0.3$, which is typical of human walking. Our test machine achieves this stride on a slope of 2.5%, and its forward speed is then 0.46 m/s, or 0.21 in units of $\sqrt{gl}$. This speed would be matched by a rimless wheel having $r_{gyr} \approx 0.5$.

Of course the wheel need not always roll at its steady speed. However, it will converge to that speed following a perturbation. In fact, small perturbations decay according to

$$\Omega_k - \Omega_0 \sim (\eta^2)^k$$ (12)

We call this decay the "speed mode," which also appears in bipedal walking. Incidentally, it is interesting to observe that convergence on a downhill slope (12) is twice as fast as deceleration on the level (6).
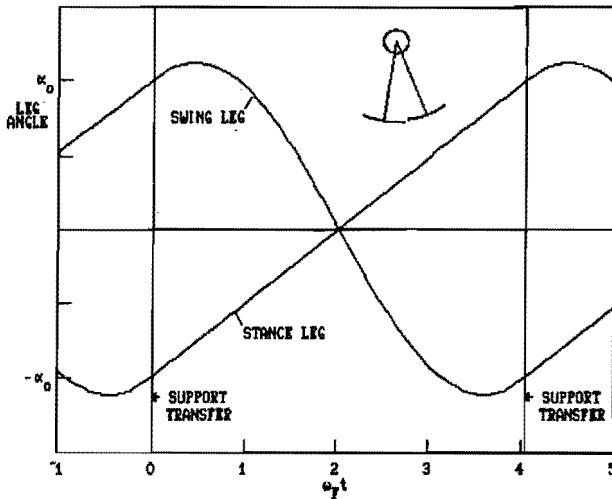
4.2. The Synthetic Wheel

In view of the poor energetics that result, it seems that rim removal is not a very progressive modification of an ordinary wheel. But perhaps improvement might be realized by making cuts elsewhere. In particular, imaging splitting the rim halfway between each spoke. Then discard all but two of the spokes, leaving a pair of legs with big semicircular feet as shown in Figure 5. Put a pin joint at the hip, and ask the following question: could the dynamics be such that while one leg is rolling along the ground, the other swings forward in just the right way to pick up the motion where the first leg leaves off?

In fact, one can devise a solution quite easily. Figure 5 shows a cycle that will continue indefinitely on level ground. The legs start with opposite angles $\pm \alpha_0$ and equal rotational speeds Ω_0, as they did in the original wagon wheel. The appropriate value for α_0 depends on Ω_0, as we will show in a moment. Since the stance leg (subscripted C for "contact") is a section of wheel, it rolls along the ground at constant speed. (Here we presume that the wheel has a large point mass at the hip; otherwise motion of the swing leg would disturb the steady rolling.) The hip (like the hub of an ordinary wheel) therefore translates steadily parallel to the ground, and so the second leg (F for "free") swings as an unforced pendulum. Then following the paths

shown in Figure 5 the legs will reach angles $\pm \alpha_0$ with speeds again equal to Ω_0. At that instant, support can roll seamlessly from one rim to the next. Thus a continuous rim has been synthesized from two small pieces.

Of course something must be done to clear the free leg as it swings forward, but we shall deal with that problem later. Also the cycle works only if the step angle α_0 is correct for the speed Ω_0; the relation is derived by matching boundary conditions. First, by inspection of the stance trajectory in Figure 5, Ω_0 must satisfy

$$\Omega_0 = \frac{2\alpha_0}{\tau_0}. \tag{13}$$

τ_0 is determined by the swing leg, which behaves as a pendulum and so follows a sinusoidal trajectory. Its formula is

$$\Delta \theta_F(\tau) = \alpha_0 \cos \omega_F \tau + \frac{\Omega_0}{\omega_F} \sin \omega_F \tau \tag{14}$$

The sinusoid passes through $\Delta \theta_F = -\alpha_0$, with speed Ω_0, when

$$\omega_F \tau_0 = 4.058 \tag{15}$$

Thus the step period for a synthetic wheel is about $\frac{2}{3}$ of the period for a full pendulum swing. Notice that this period is independent of α_0. The speed (13) is then

$$\Omega_0 = \frac{2\omega_F \alpha_0}{4.058} \tag{16}$$

Thus to change the speed of a synthetic wheel, change α_0 (i.e., the length of the step), while τ_0 remains constant —determined solely by the leg's inertial properties and gravity g.

Of course the synthetic wheel is contrived for convenient analysis, but the results have broader application. Our test machine has similar behavior. Figure 6 shows that its step period is fairly insensitive to step length; moreover $\tau_0 \approx 2.8$ in units of $\sqrt{l/g}$ and $\omega_F \approx 1.39$, so $\omega_F \tau_0 \approx 3.9$, which is quite close to the value given by (15). However, (15) is not so accurate for human walking; my own pendulum period, measured by standing on a ledge and dangling one leg, is ≈ 1.4 s,

parameters as listed on the plot. The analysis matches experiment poorly if no allowance is made for rolling friction (T_C), but reasonable consistency is realized if the friction is taken to be 0.007 mgl. With this level of friction, walking is calculated to be unstable on slopes less than 0.8%.
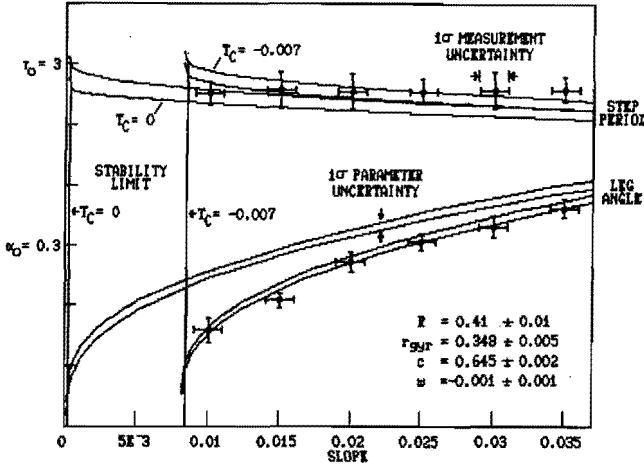
and my step period varies from ≈ 0.55 s at low speed to ≈ 0.50 s at high speed. Thus the ratio of step period to pendulum period is ≈ 0.36 to ≈ 0.39, as opposed to 0.65 for the wheel (15). I have significantly more life in my stride than either the wheel or our test biped!

While Figure 5 shows that a synthetic wheel is possible in theory, can its cycle actually be realized in practice? This boils down to an issue of stability, and it turns out that the synthetic wheel is just as stable as an ordinary wheel. That is, both have neutrally stable "speed modes"; in the case of a synthetic wheel, a change in speed leads to a new α_0 according to (16). In addition, the synthetic wheel has two other "step-to-step" modes that prove to be stable; these are discussed in section 8.

5. Steady Walking of a General 2D Biped

The biped of Figure 2 is similar to the synthetic wheel but allows for broader variation of parameters. Adjustable parameters include

1. Foot radius R
2. Leg radius of gyration r_{gyr}

3. Leg center of mass height c
4. Fore/aft center of mass offset w
5. Hip mass fraction m_H

We will examine the effects of varying each parameter.

Our calculations of gait and stability rely on step-to-step (S-to-S) analysis, which is explained as follows. At the start of a step, say the kth, the legs have equal and opposite angles $\pm\alpha_k$ and rotational speeds Ω_{Ck}, Ω_{Fk}. The motion proceeds roughly as for the synthetic wheel, with appropriate arrangements to prevent toe-stubbing at mid-stride. The step ends when leg angles are again equal and opposite, but in general different (say α_{k+1}) from α_k. At that point the swing foot hits the ground, and the leg speeds change instantaneously to their initial values for the following step Ω_{Ck+1}, Ω_{Fk+1}. We will formulate equations relating $(\alpha_k, \Omega_{Ck}, \Omega_{Fk})$ to $(\alpha_{k+1}, \Omega_{Ck+1}, \Omega_{Fk+1})$. We will then use these to find naturally repeating initial conditions (i.e., passive cycles) and to examine how perturbations evolve from step to step.

5.1. Start- to End-of-Step Equations

During the step the machine is supported on one foot, and its state is specified by the two leg angles θ_C, θ_F, and the speeds Ω_C, Ω_F. In general the equations of motion are nonlinear in these variables, but since in walking the legs remain near the vertical and the speeds remain small ($\ll \sqrt{g/l}$), linearization is justified. Thus the linearized equations are

$$\mathbf{M}_0 \begin{bmatrix} \dot{\Omega}_C \\ \dot{\Omega}_F \end{bmatrix} = \mathbf{M}_0 \dot{\mathbf{\Omega}} = \mathbf{T} \tag{17}$$

The inertia matrix $\mathbf{M}_0$ is derived in the appendix (65). $\mathbf{T}$ lists the torques about the stance foot and hip. It can include friction or control inputs, but for our machine the principal torque is gravitational:

$$\mathbf{T}_g = \mathbf{K}[\Delta\theta_{SE} - \Delta\theta] \tag{18}$$

The stiffness matrix $\mathbf{K}$ and equilibrium position $\Delta\theta_{SE}$ are also derived in the appendix [eqs. (52), (53), (54)].

$\Delta\theta$ is the rotation from the surface normal. For small γ, $\Delta\theta_{SE}$ can be written as

$$\Delta\theta_{SE} = \Delta\theta_W + \mathbf{b}\gamma \qquad (19)$$

By way of explanation you can imagine that if the feet were points (i.e., zero foot radius) then the equilibrium position would be legs-vertical, which means that both elements of $\mathbf{b}$ would be -1. However with non-zero foot radius the stance leg would have to rotate past the vertical to put the overall mass center over the contact point, so $b_1 < -1$. Also moving the legs' mass centers fore and aft from the leg axes (i.e., nonzero w, Fig. 2) would make for nonvertical equilibrium even on level ground, and this is handled by $\Delta\theta_W$.

Putting the gravitational torque (18) into the equations of motion (17) leaves a fourth-order linear system. This can be solved to jump from the start-of-step to any later time, via a 4×4 transition matrix $\mathbf{D}$:

$$\begin{bmatrix} \Delta\theta(\tau_k) \\ \Omega(\tau_k) \end{bmatrix} = \mathbf{D}(\tau_k) \begin{bmatrix} \Delta\theta_k - \Delta\theta_{SE} \\ \Omega_k \end{bmatrix} + \begin{bmatrix} \Delta\theta_{SE} \\ 0 \end{bmatrix}. \qquad (20)$$

The elements of $\mathbf{D}$ for a given $\mathbf{M_0}$, $\mathbf{K}$, and τ_k are calculated by standard methods for linear systems. For transition to the end-of-step, τ_k must be chosen so that the elements of $\Delta\theta(\tau_k)$ are equal and opposite. Thus define

$$\lambda = \begin{bmatrix} -1 \\ 1 \end{bmatrix}. \qquad (21)$$

Then

$$\Delta\theta_k = \lambda\alpha_k, \qquad (22)$$

$$\Delta\theta(\tau_k) = -\lambda\alpha_{k+1}. \qquad (23)$$

5.2. Support Transfer

When (23) is satisfied, foot strike occurs, which as for the rimless wheel we treat as an inelastic collision. In this case two conditions apply:

1. Conservation of angular momentum of the whole machine about the point of collision, as for the rimless wheel (3).
2. Conservation of angular momentum of the trailing leg about the hip.

These are expressed mathematically as

$$\mathbf{M^+\Omega^+} = \mathbf{M^-\Omega^-}, \qquad (24)$$

where "$-$" and "$+$" respectively denote pre- and post-support transfer. The inertia matrices $\mathbf{M^-}$ and $\mathbf{M^+}$ depend on the leg angles at foot strike, as discussed in the appendix [eqs. (65), (68)]. The ordering of Ω may be confusing, since the stance and swing legs exchange roles at support transfer. We adopt the convention that the first element of Ω refers to the *post*-transfer stance leg. Hence the pre-transfer indexing must be flipped:

$$\Omega^- = \begin{bmatrix} 0 & 1 \\ 1 & 0 \end{bmatrix} \Omega(\tau_k) \equiv \mathbf{F}\Omega(\tau_k). \qquad (25)$$

From (24), then, the initial speeds for step $k+1$ are

$$\Omega_{k+1} = \mathbf{M^{+-1}M^-F}\Omega(\tau_k) \equiv \Lambda\Omega(\tau_k). \qquad (26)$$

5.3. "S-to-S" Equations

Combining the start- to end-of-step equation (20) with the foot strike conditions [eqs. (22), (23), (26)] produces the S-to-S equations. It is convenient to break $\mathbf{D}$ in (20) into 2×2 submatrices, so the system is written as

$$-\lambda\alpha_{k+1} = \mathbf{D}_{\theta\theta}[\lambda\alpha_k - \Delta\theta_{SE}] + \mathbf{D}_{\theta\Omega}\Omega_k + \Delta\theta_{SE}, \qquad (27)$$

$$\Omega_{k+1} = \Lambda\mathbf{D}_{\Omega\theta}[\lambda\alpha_k - \Delta\theta_{SE}] + \Lambda\mathbf{D}_{\Omega\Omega}\Omega_k. \qquad (28)$$

Bear in mind that while formulation of this set has been simple, evaluation is not quite so straightforward. Given initial conditions (α_k, Ω_k), the time τ_k (which determines $\mathbf{D}$) at which the leg angles are next equal and opposite must be determined. Then α_{k+1} (27)

Fig. 7. Step period and angle measured at heel strike in trials of the test biped. The machine was started by hand on a 5.5-m ramp inclined at 2.5% downhill, and after a few steps settled into a fairly steady gait. Dots show the mean values, and bars the scatter recorded over six trials. Lengths are normalized by leg length l, and periods by $\sqrt{l/g}$. "C" denotes start-of-stance on the center leg; "O" on the outer legs.
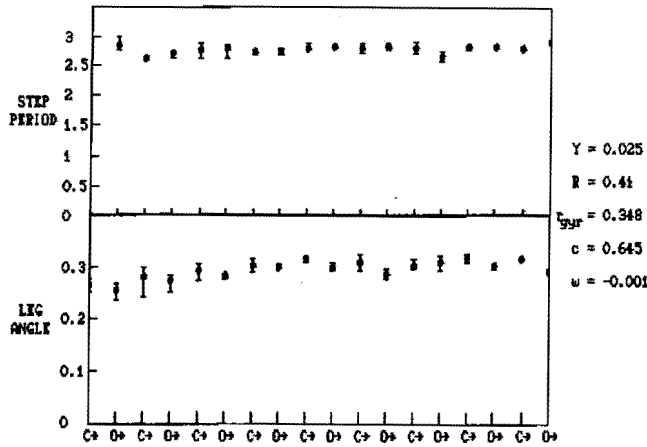
determines Λ (26), which in turn allows evaluation of Ω_{k+1} (28).

5.4. Solution for the Walking Cycle

For cyclic walking, initial conditions must repeat from step to step:

$$\alpha_{k+1} = \alpha_k = \alpha_0, \qquad (29)$$

$$\Omega_{k+1} = \Omega_k = \Omega_0. \qquad (30)$$

Imposing these conditions on S-to-S equations (27) and (28) leads to a compact solution for the walking cycle. First solve for Ω_0 using (28):

$$\Omega_0 = [I - \Lambda D_{\Omega\Omega}]^{-1} \Lambda D_{\Omega\theta}[\lambda\alpha_0 - \Delta\theta_{SE}]. \qquad (31)$$

Then substitute for Ω_0 in (27); the end result can be written as follows. Define

$$D'(\alpha_0, \tau_0) = D_{\theta\theta} + D_{\theta\Omega}[I - \Lambda D_{\Omega\Omega}]^{-1} \Lambda D_{\Omega\theta}. \qquad (32)$$

Then (27) can be written as

$$0 = [D' - F]\lambda\alpha_0 - [D' - I]\Delta\theta_{SE}$$
$$= [D' - F]\lambda\alpha_0 - [D' - I][\Delta\theta_W + b\gamma]. \qquad (33)$$

The last line follows from (19). This is the steady-cycle condition, with two equations in three variables α_0, τ_0, and γ. Usually we specify α_0 and solve for the other two. Equation (33) then has either two solutions or none. If two, then one cycle has $\omega_F\tau_0 < \pi$, and is invariably unstable. The other corresponds to a synthetic-wheel–like cycle with $\omega_F\tau_0$ between π and $3\pi/2$. This is the solution of interest. Thus we use the synthetic-wheel estimate (15) to start a Newton's method search for τ_0, and if a solution exists, then convergence to five significant figures requires about five iterations.

6. Steady Walking of the Test Machine

The analytical solution for steady walking is compared with experiment in Figure 6. Experimental data were obtained by multiple trials as shown in Figure 7; in each trial our test biped was started by hand from the top of a ramp, and after a few steps it settled into the steady gait appropriate for the slope in use. (Notice, incidentally, that the rate of convergence is a measure of stability; we will pursue this analytically in the next section.) Several trials were done on each slope, and means and standard deviations for α_0 and τ_0 were calculated over all data except those from the first few steps of each trial.

Our predictive ability to compare with analysis was limited by uncertainty in the machine's parameters. Each leg's center-of-mass height c was measured to about 1 mm by balancing each leg on a knife edge; w to about 0.5 mm by hanging each leg freely from the hip; and r_{gyr} to about 2.5 mm by timing pendulum swings. The center and outer legs were ballasted to match within these tolerances and differed in mass by only a few grams (i.e., $\approx 0.001\ m$).

When these parameters were put into (33) we found (as Figure 6 indicates) that the observed cadence was slower than predicted. We suspected that the discrepancy was caused by rolling friction on the machine's rubber-soled feet. Hence we added a constant to the first element of T in (17), which modified $\Delta\theta_W$ in (19). A value of -0.007 brought the analytical results into line with observation. In dimensional terms this is equivalent to 25 gm-force applied at the hip. We could

not devise an independent measurement of rolling friction, but this figure is credible.

However, after adjusting friction for a reasonable fit, we still found a discrepancy in that the observed step period is less sensitive to speed than the analysis indicates. We therefore suspected that the inelastic model for foot strike was imprecise, and in fact there was a bit of bouncing at high speed. But in any case the residual discrepancy is small, so our current S-to-S equations (27) and (28) apparently form a sound basis for further investigation, in particular of stability and parametric variations.

Here the efficiency of biped walking should be noted. For comparison with other modes of transport, we measure efficiency by specific resistance:

$$SR \equiv \frac{\text{resistive force}}{\text{weight}} = \frac{\text{mechanical work done}}{\text{weight} \times \text{distance travelled}}$$

For a vehicle powered by descending a slope, SR is just equal to γ, or about 2.5% for our machine using $\alpha_0 \approx 0.3$, which is comfortable for humans. This figure would be terrible for a car, but it is very good in comparison with other rough-terrain vehicles such as multilegged crawlers and bulldozers (Waldron 1984).

7. Linearized Step-to-Step Equations

A cyclic solution is a necessary but not quite sufficient condition for practical passive walking. The walking cycle must also be *stable*. Stability can be assessed by linearizing eqs. (27) and (28) for small perturbations on the steady gait. The transition matrix D and the support transfer matrix Λ can be approximated for this purpose as follows:

$$\mathbf{D}(\tau_k) \approx \mathbf{D}(\tau_0) + \frac{\partial \mathbf{D}}{\partial \tau}(\tau_k - \tau_0), \qquad (34)$$

$$\Lambda(\alpha_{k+1}) \approx \Lambda(\alpha_0) + \frac{\partial \Lambda}{\partial \alpha}(\alpha_{k+1} - \alpha_0). \qquad (35)$$

After substituting these into (27) and (28) and mani-

Table 1. S-to-S Eigenvectors of the Test Machine on a 2.5% Slope

Mode	Speed	Swing	Totter
Eigenvalue, z	0.70	−0.05	−0.83
$\alpha - \alpha_0$	1	1	1
$\Omega_C - \Omega_{C0}$	1.1	1.1	0.12
$\Omega_F - \Omega_{F0}$	0.30	7.3	−0.03

pulating to collect terms, we are left with the following approximate form of the S-to-S equations:

$$\begin{bmatrix} \alpha_{k+1} - \alpha_0 \\ \Omega_{Ck+1} - \Omega_{C0} \\ \Omega_{Fk+1} - \Omega_{F0} \\ \tau_k - \tau_0 \end{bmatrix} = \mathbf{S} \begin{bmatrix} \alpha_k - \alpha_0 \\ \Omega_{Ck} - \Omega_{C0} \\ \Omega_{Fk} - \Omega_{F0} \end{bmatrix}. \qquad (36)$$

The formula for S is given in the appendix [eqs. (69), (70), and (72)]. The important point here is that S is the transition matrix of a standard linear difference equation, so the eigenvalues of its upper 3 × 3 block indicate stability [the equation for $(\tau_k - \tau_0)$ is ancillary]. If all have magnitude less than unity, then the walking cycle is stable; the smaller the magnitude, the faster the recovery from a disturbance. (If, however, the walking cycle is unstable, then linearized S-to-S equations are helpful for design of a stabilizing control law. This was in essence the approach of Miura and Shimoyama (1984). See also McGeer (1989) for active stabilization of a passive cycle.)

8. S-to-S Modes of the Test Machine

Results of stability analysis for our test biped are listed in Table 1. Similar results are found over a wide range of parameter variations, so the modes can be considered typical for passive walking.

The "speed mode" is analogous to the transient behavior of a rimless wheel, with z corresponding to η^2 in (12). The eigenvalue is linked to energy dissipation at support transfer. Thus for the synthetic wheel, $z = 1$ in this mode (i.e., stability is neutral with respect to speed change), as we noted earlier.

The "swing mode" is so named because the eigenvector is dominated by Ω_F. The eigenvalue of this mode is usually small, and in fact reduces to zero in the synthetic wheel, which means that a "swing" perturbation is eliminated immediately at the first support transfer. Physically this occurs because the posttransfer speed of the synthetic wheel's legs is determined entirely by the momentum of the large hip mass; the pretransfer Ω_F is irrelevant.

Finally, the "totter mode" is distinguished by a negative eigenvalue, which means that perturbations alternate in sign from one step to the next. Again the synthetic wheel offers an easily understood special case. Since the wheel cannot dissipate energy, it retains its initial rolling speed for all time. If the initial step angle is not appropriate to the initial speed as specified by (13), then the angle must accommodate through some sort of transient, which turns out to be the totter mode. The eigenvalue can be found analytically by generalizing the swing trajectory formula (14) for $\alpha_k \neq \alpha_0$:

$$-\alpha_{k+1} = \alpha_k \cos \omega_F \tau_k + \frac{\Omega_0}{\omega_F} \sin \omega_F \tau_k. \qquad (37)$$

Meanwhile the generalized stance trajectory [cf. (13)] is

$$\alpha_{k+1} = -\alpha_k + \Omega_0 \tau_k. \qquad (38)$$

Now differentiate eqs. (37) and (38) with respect to α_k:

$$-\frac{d\alpha_{k+1}}{d\alpha_k} = \cos \omega_F \tau_k$$
$$+ (-\alpha_k \omega_F \sin \omega_F \tau_k + \Omega_0 \cos \omega_F \tau_k) \frac{d\tau_k}{d\alpha_k} \qquad (39)$$

$$\frac{d\alpha_{k+1}}{d\alpha_k} = -1 + \Omega_0 \frac{d\tau_k}{d\alpha_k} \qquad (40)$$

Solving for the derivatives and evaluating at τ_0 gives

$$\frac{d\alpha_{k+1}}{d\alpha_k} = -\frac{4 \cos \omega_F \tau_0 - \omega_F \tau_0 \sin \omega_F \tau_0}{2 + 2 \cos \omega_F \tau_0 - \omega_F \tau_0 \sin \omega_F \tau_0} = -0.20, \qquad (41)$$

$$\frac{d\tau_k}{d\alpha_k} = \frac{1}{\Omega_0} \frac{2 - 2 \cos \omega_F \tau_0}{2 + 2 \cos \omega_F \tau_0 - \omega_F \tau_0 \sin \omega_F \tau_0} = \frac{0.80}{\Omega_0}. \qquad (42)$$

It follows from (41) that perturbations converge exponentially according to

$$\alpha_k - \alpha_0 \sim -0.2^k \quad \text{in the totter mode} \qquad (43)$$

In summary then, and with some oversimplification for clarity, the "speed" mode in passive walking is a monotonic convergence to the speed appropriate for the slope in use. The "swing" mode is a rapid adjustment of the swing motion to a normal walking pattern. The "totter" mode is an oscillatory attempt to match step length with forward speed. An arbitrary perturbation will excite all three modes simultaneously. Of the three, the totter mode differs most between the synthetic wheel and our test biped ($z = -0.2$ vs. -0.83), and our parametric surveys indicate that it bears watching. We will show examples of parameter choices that make the totter mode unstable.

9. Larger Perturbations

The preceding analysis applies only for small perturbations, but an obvious question is, "How small is small?" There is a limit: if the machine were started just by standing the legs upright and letting go, it would fall over rather than walk! Thus starting requires a bit more care. In general, the machine could be released with arbitrary leg angles and speeds, and it would be nice to know the "convergence zone" in the four-dimensional state space. Unfortunately the boundary of a 4D volume is rather difficult to map, so we have restricted attention to finding the maximum tolerable perturbation in the initial Ω_C or Ω_F. This is done by serial evaluation of the nonlinear S-to-S equations (27) and (28). The results show that Ω_F can vary over wide limits (e.g., <0 to $>+150\%$ of the cyclic value). However, Ω_C is sensitive; many passive walkers can only tolerate an error of a few percent in the starting speed. Still this is not so exacting as it sounds; manual starting (by various techniques) is quite natural, and success is achievable with little or no practice. Furthermore, the boundaries of the convergence zone are sharp, and if the machine starts even barely inside

the edge it settles to the steady cycle very nearly as suggested by the small-perturbation analysis.

An alternative to the convergence-zone measure of robustness is resistance to jostling. Thus we calculated transients produced by disrupting the steady gait with a horizontal impulse, applied at the hip just as the legs passed through $\Delta\theta = 0$. As an intuitive standard of reference, we compared the walker with a similar machine resting with legs *locked* at $\pm\alpha_0$. It turns out that a passive walker can tolerate a useful fraction of the impulse required to topple the locked machine; the level varies widely with choice of machine parameters, but 25% (forward or backward) is representative. The calculation has to be done carefully, since bands of tolerable and intolerable impulse magnitudes are interspersed. Twenty-five percent is a typical upper bound for the first tolerable band. More aggressive jostling would have to be countered by active control.

The jostling calculation was particularly helpful in dispelling the inclination to associate robustness with rapid convergence from small perturbations. In fact, a biped with a slowly convergent or even slightly unstable totter mode may well tolerate a stronger midstride jostle than a machine with better totter stability. Thus a practical biped designer might be willing to accept a requirement for "weak" active stabilization of the steady cycle in return for better resistance to knockdowns.

m, l, or g). Quite simply, changing m scales the forces but doesn't change the gait. Changing l scales the step period by $1/\sqrt{l}$, and the speed by $\sqrt{l}$. Changing g scales both period and speed by $\sqrt{g}$. A noteworthy consequence was experienced by the lunar astronauts in 1/6th Earth's gravity. Apparently they had a sensation of being in slow motion, and indeed walking could achieve only 40% of normal speed. Rather than accept that, they hopped instead (McMahon 1984).
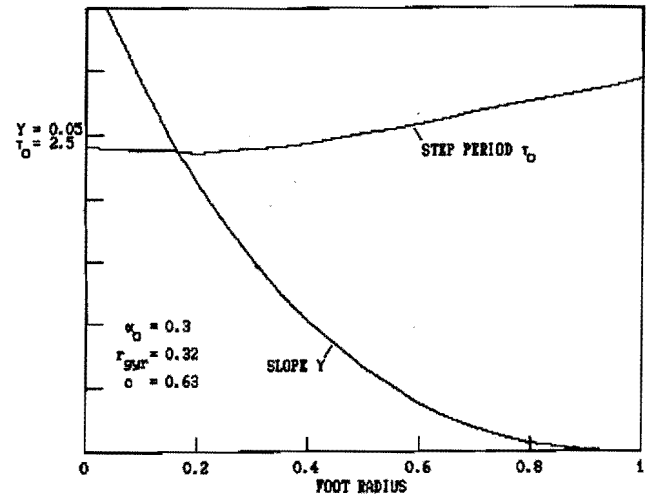
10. Effect of Parameter Variations

We now embark on a brief survey of the effect of design variables on walking performance. Our purpose is twofold: first, to outline the designer's options, and second, to illustrate that walking cycles can be found over a wide range of variations on the 2D biped theme.

10.1. Scale

Before discussing variation of dimensionless parameters we should note the effect of scale (i.e., changing
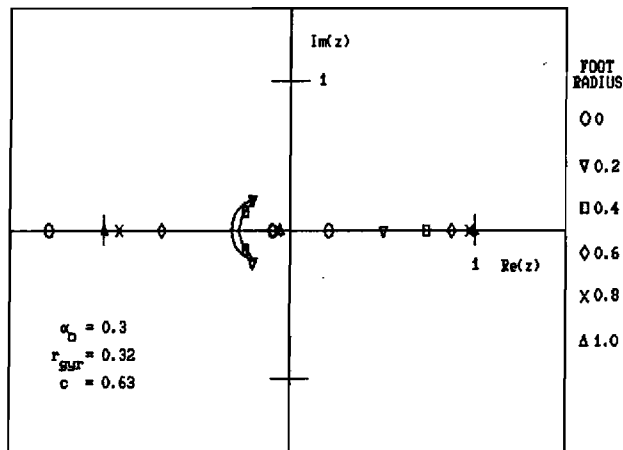
10.2. Foot Radius

Figure 8 shows an example of the effect of foot radius on steady walking. Most notable is the improvement in efficiency as the foot changes from a point to a section of wheel. Thus with $R = 0$ we have a biped that, like the rimless wheel, needs a relatively steep slope, and with $R = 1$ we have a synthetic wheel rolling on the level.

Figure 9 shows the locus of S-to-S eigenvalues as a function of R. The speed eigenvalue increases from $z \approx 0.2$ with a point foot to $z = 1$ (i.e., neutral speed stability) with a wheel; this is associated with the improvement in efficiency and is consistent with (12). Meanwhile the totter and swing modes are well separated with a point foot, but coupled with mid-sized

Fig. 9. Locus of the three step-to-step eigenvalues for the walking cycles plotted in Fig. 8, with foot radius as the parameter. In this example one eigenvalue (for the "totter mode") lies outside the unit circle if the feet are very small; this indicates that passive walking is unstable. However, with other choices for c and r_{gyr}, walking is stable even on point feet.

Fig. 10. Variation of the walking cycle with c, the height of the leg's mass center. |z| is the magnitude of the totter mode eigenvalue; here it indicates that passive walking is unstable for bipeds with c too low or too high. (The kinks appear where z branches into the complex plane, as in Fig. 9.) The high-c problem arises because of excessively long swing-pendulum periods, while the low-c problem is caused by inefficient support transfer. The latter can be remedied by adding mass at the hip. In this example, m_H is zero.

feet so that the two eigenvalues form a complex pair. Then with larger foot radius they separate again, and $R = 1$ puts the totter eigenvalue near $z = -1$. [A true synthetic wheel has $z = -0.2$ (43), but its hip mass is much larger than specified in this example.] The big-footed bipeds in this example thus have relatively weak totter stability, but it still turns out that their resistance to jostling is better than with small feet.
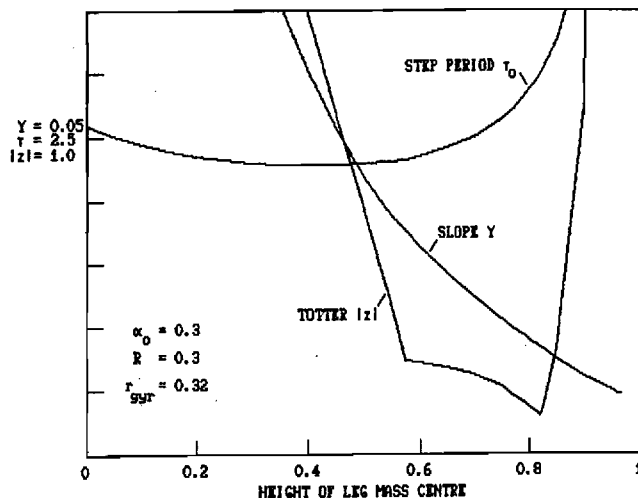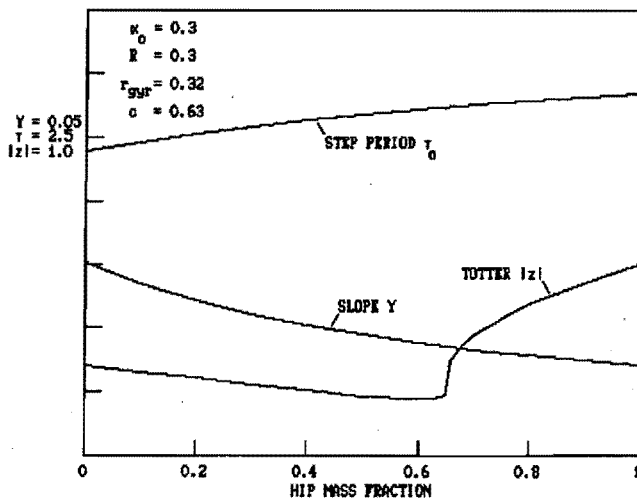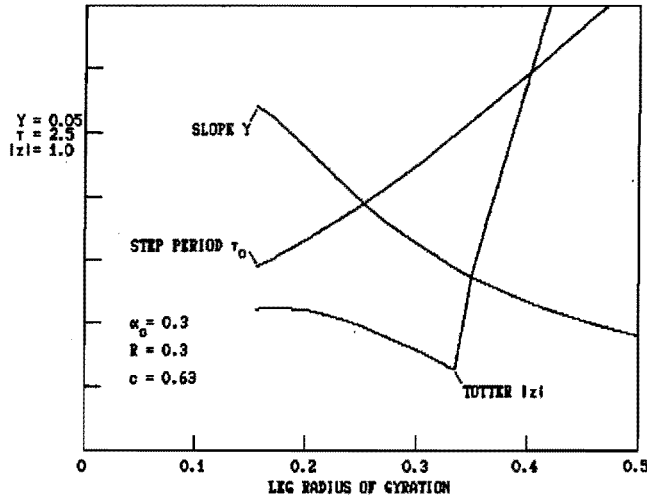
We should mention that the semicircular foot is a mathematical convenience rather than a physical necessity; doubtless other arrangements are feasible. For example, a flat foot could be used on which support would transfer impulsively from heel to toe at mid-stride. Walking would be less efficient than with a curved foot, but apart from that we would expect a similar passive gait. For comparison with a circular foot, the key feature is translation of the support point during stance, which is $2\ \alpha_0 R$. Thus a human, with heel-to-ball distance of $\approx 0.2\ l$ and a typical stride angle of $\alpha_0 = 0.3$, has an "equivalent radius" of ≈ 0.3.

swing leg can't come forward in time to break the fall of the stance leg, and the walking cycle vanishes. On the other hand, lowering r_{gyr} or c causes a different problem: support transfer becomes inefficient according to (5). [Note that α_0 in (5) is the angle subtended by the feet, at the overall mass center.] If the efficiency is too poor, then the cycle becomes unstable or even vanishes entirely, as in the example of Figure 11. However, the situation can be retrieved by adding mass at the hip, which raises the overall mass center and thus improves efficiency. A human has about 70% of body mass above the hip; this is sufficient to make support transfer efficient regardless of leg properties.

10.3. Leg Inertia and Height of the Mass Center

Leg radius of gyration and center-of-mass height have similar effects, as illustrated in Figures 10 and 11. Increasing r_{gyr}, or raising c with r_{gyr} held constant, lengths the pendulum period and so slows the cadence (15). If the mass center is too close to the hip, then the

10.4. Hip Mass

Figure 12 illustrates the effect of adding point mass at the hip. Efficiency improves, and it turns out that jostling resistance improves as well. Still more advantage can be gained if the mass is in the form of an extended torso. For example, the torso can be held in a backward recline, reacting against the stance leg; the reaction provides a braking torque that allows a steep descent. Analysis of this scheme and other roles of the torso is reported by McGeer (1988).

Fig. 11. Leg inertia and c have similar effects on the walking cycle, as indicated by comparing this plot with Fig. 10. The effects here are also mediated by the swing pendulum frequency and by the efficiency of support transfer.

Fig. 12. Our test biped is just a pair of legs, but passive walking also works while carrying a "payload" at the hip. Actually the added mass improves efficiency of the walking cycle.

Fig. 13. Passive walking is forgiving of most parameter variations, but even a small amount of friction in the hip joint can destroy the cycle. However, walking can be restored by moving the legs' mass centers backward from

the leg axes (w < 0, Fig. 18) as long as the friction is only moderate. For this example we have used a viscous model for friction, which is measured by the damping ratio for pendulum oscillations of the swing leg.

chanical arrangements, for instance those made by bone and cartilage, may not be quite as good. Fortunately, compensation can be made by lateral offset (w) of the legs' mass centers from the axes. Thus, as Figure 13 indicates, if the joint has significant friction, then the designer should shift the leg mass backward from the line between hip and foot center of curvature (i.e., $w < 0$).

Actually w is a powerful remedy for a variety of similar ailments (McGeer 1988; 1989). But like any powerful medicine it must be treated with some care. Figure 14 shows that for any given set of machine parameters, w must be set within narrow limits if passive walking is to work. Experiments bring the point home; changing w by only a few millimeters has a very noticeable effect on the feel of manual starting. The power of w makes it attractive not only as a design parameter but also as a *dynamically adjustable* control variable; it might be used, for example, to modulate the gait from one step to the next.
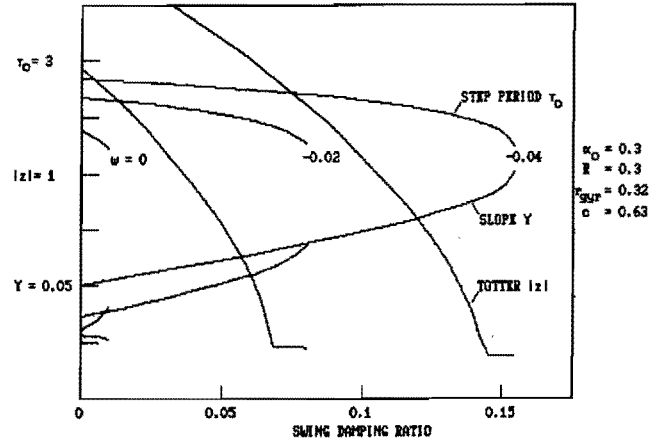
10.5. Hip Damping and Mass Offset

The last few examples have indicated that passive walking is robust with respect to parametric variations. However, it is not universally tolerant, and the hip joint is particularly sensitive. As shown in Figure 13, introducing only a small amount of friction makes the cyclic solution vanish. Consequently, in our test biped we use ball bearings on the hip axle, and these keep the friction acceptably low. However, alternative me-

10.6. Leg Mismatch

To close this section on parametric effects, we present a curiosity that may have some implication for the study of gait pathology. Since our biped's legs could not be matched precisely, we were concerned about the sensitivity to differences between them. By way of

74

Fig. 14. Experiments confirm the powerful effect of mass offset w on the walking cycle. (w was adjusted by shifting the feet relative to the legs.) With each setting we did a series of trials as in Fig. 7. α_0 and τ_0 are well matched by calculations if T_C is taken to be -0.007, but then walks that were in fact sustained for the full length of three six-foot tables are calculated to be unstable. Taking T_C to be zero gives a better match to the observed stability, but leaves relatively large discrepancies in α_0 and τ_0. We suspect that our support transfer model is imprecise, but in any case the sensitivity to w is clear.

Fig. 15. The stable cycle calculated for a biped having legs with a 10% mass mismatch. m_C is the mass of the stance leg. Each step is similar to that of a synthetic wheel, but the cycle repeats over four steps rather than one. (With smaller mismatch the cycle repeats in two steps.)
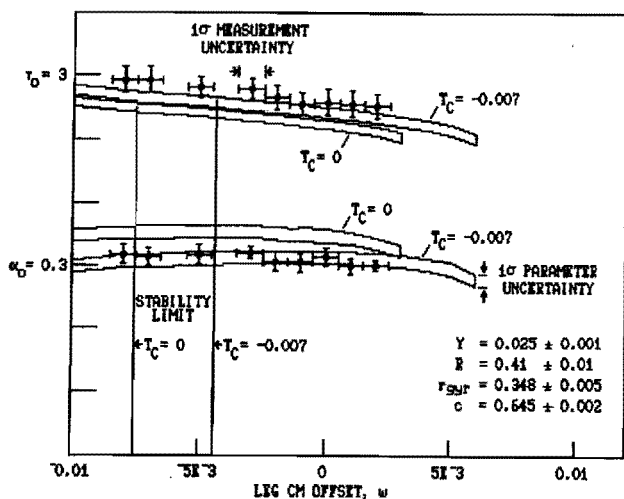
investigation we calculated walking cycles with legs of different mass. The steady-walking solution (33) doesn't apply with mismatched legs, so instead we did serial calculations with S-to-S equations (27) and (28) until a steady gait emerged. With a small mismatch, the cycle repeats in two steps (as would be expected). But with larger mismatch, the stable cycle repeats in four steps, as plotted in Figure 15. Here, then, is an example of frequency jumping, which is not uncommon in nonlinear systems.
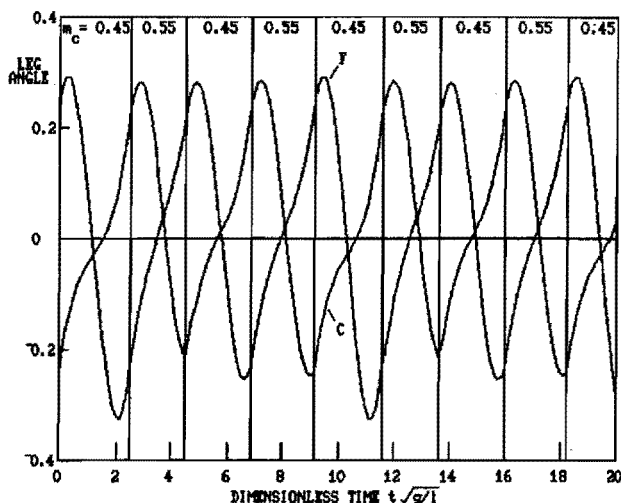
11. Fully Passive Walking

We mentioned earlier that our 2D, stiff-legged model allows simple analytical treatment of walking, but it forces resort to inelegant methods of clearing the swing foot. Fully passive foot clearance would be preferable; we will discuss two options.

11.1. Rocking

The toy of Figure 1, and its quadrupedal cousins, clear swing feet by lateral rocking. The frontal view shows the key design feature, which is that the feet are approximately circular in lateral as well as longitudinal section, and have approximately coincidental centers of curvature. The center of curvature is above the center of gravity, which makes lateral rocking a pendulum oscillation.

We have analyzed the combination of rocking with 2D synthetic wheel dynamics, under the approximation of zero yaw (i.e., that the hip axle remains normal to the direction of motion). This is exactly true for quadrupedal toys and seems fairly accurate for the biped. The rocking frequency must be tuned to the swing frequency, such that half a rocking cycle is completed in one step. Hence the ratio of swing to rocking frequencies, from (15), should be

$$\frac{\omega_F}{\omega_R} = \frac{4.058}{\pi}. \qquad (44)$$

If this condition is satisfied, then rocking and swinging naturally phase-lock at the first support transfer, and thereafter walking is non-dissipative. However, if the condition is not satisfied, then the phasing must be "reset" on each step; this entails an energy loss. If the mistuning is too large, then there is no cycle at all.

An additional problem arises if the feet have non-zero lateral separation. Then support transfer bleeds energy out of the rocking motion via the rimless-wheel mechanism (3). But it turns out that, at least in the

zero yaw approximation, only a small amount of energy can be regained from forward motion (i.e., by descending a steeper hill). Hence passive walking cannot be sustained unless the foot spacing is quite small.

These constraints of frequency tuning and lateral foot spacing reduce the designer's options, and moreover produce a machine that is inevitably rather tippy from side to side. Hence rocking is unattractive for a practical biped, but it remains a wonderful device for the toy.

11.2. Knees

Of course we humans rock as we walk, but only for lateral balance; for foot clearance we rely on knee flexion. Mochon and McMahon (1980) demonstrated that this motion might well be passive. The key result of the study is that if a straight stance leg and knee-jointed swing leg are given initial conditions in an appropriate range, then they will shift ballistically from start- to end-of-step angles. Recently we have found that support transfer can then regenerate the start-of-step conditions, thus producing a closed passive cycle.
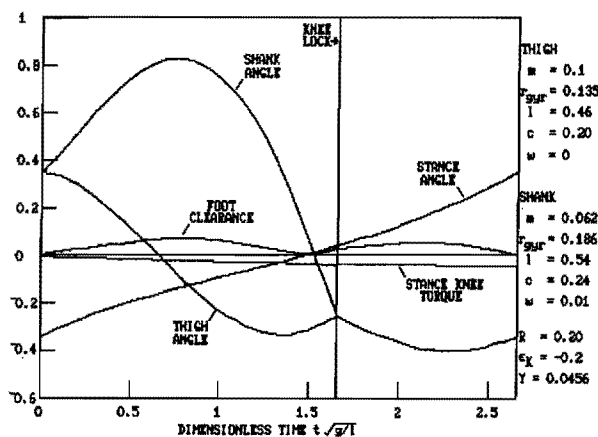
A full discussion of passive walking with knees must be left for a future report, but here we will review one example as shown in Figure 16. The model is still a 2D biped, but with pin-jointed knees and mechanical stops, as in the human knee, to prevent hyperextension. As in ballistic walking, the stance knee is *specified* to remain locked against the stop throughout the step, while the swing knee is initially free and flexes passively as plotted in Figure 16. Then it re-extends and hits the stop. (As always we treat the collision as impulsive and inelastic.) Thereafter both knees remain locked until foot strike.

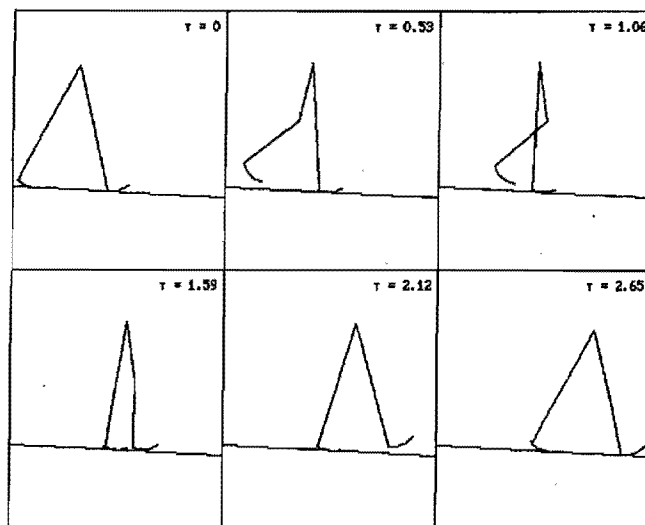Parametric studies of this knee-jointed model have produced these results:

1. Passive cycles are found over parameter ranges more limited than those in stiff-legged walking, but still quite broad.
2. With proper choice of parameters, naturally arising torques keep the stance and swing knees locked through the appropriate phases of the cycle.

Fig. 16. Our test biped has rigid legs, but passive walking also works with knees. The parameters here are quoted according to the convention of Fig. 18 and are similar to those of a human (including $m_H = 0.676$). (A) Flexure of the swing knee takes care of foot clearance (although just barely). Meanwhile a naturally generated torque holds the stance knee locked against a mechanical stop. (ϵ_K is the angle from the locked knee to the foot's center of curvature.) (B) The motion is obviously similar to human walking, but it is slower; the period of this cycle would be ≈ 0.85 s for a biped with 1-m leg length. There is also a faster cycle, but we prefer the slower because it turns out to be stable and more efficient.

A

B

3. A passive cycle with knee joints is possible only if the foot is displaced forward relative to the leg, as shown in Figure 16. The implication is that humans might have difficulty if their feet didn't stick out in front of their legs.
4. A large fraction of the swing leg's kinetic energy is dissipated at knee lock, and therefore

76

knee-jointed walking is less efficient than stiff-legged walking. To keep the penalty small, the swing leg's energy must be small compared with the total energy of motion. This implies that most of the mass should be above the hip.

On the last point it might be argued that foot clearance with knees seems inefficient, whereas *active* retraction can in principle consume no energy at all. However, in practice economical food retraction may be hard to achieve. Our test biped has a "fundamental" dissipation (from Figure 6) of ≈ 0.2 J per step, while the tiny motors that lift its feet waste ≈ 3 J per step! Some goes into friction in the leadscrews, and some into switching transistors. At this rate, passive knee flexion is a bargain, and moreover a small active intervention at the right time may reduce the knee-locking loss substantially.

12. Action on Passive Walking

Having surveyed the physics of passive walking, our next objective must be exploitation of the effect to make machines with some practical capability. We see developments proceeding as follows:

1. "Powered" passive walking on shallow up- and downhill slopes in 2D
2. Step-to-step gait modulation over unevenly-spaced footholds in 2D
3. Walking on steep slopes, stairs, and 2D rough terrain
4. Lateral balance and steering

We are presently building a machine to test the first two developments. It will be similar to the first biped, but with 1-m leg length and a torso. Power will be provided by pushing with the trailing leg as it leaves the ground. (This is analogous to plantar flexion in humans, but the implementation is quite different.) Gait modulation is to be done by applying torques between the legs and torso. McGeer (1988) presents the analytical basis for this machine, as well as alternative options for applying power and control. S-to-S treatment is a key principle; thus control laws look at the state of the machine only once per step. This ap-

proach proves attractively simple, both mathematically and mechanically.

We have yet to proceed to the next problem of walking with steep changes in elevation. One promising strategy is to seek passive fore/aft leg swinging that can proceed in synchrony with actively cycled variation in leg length. This approach works on shallow slopes, with the length adjustments serving as a source of energy (McGeer 1988). However, further results await reformulation of equations of motion (17) and (18), since the linearization used here is invalid on steep slopes.

Finally, we expect that lateral balance will have to be done actively. One possibility is to control as when standing still (i.e., by leaning in appropriate directions). Another scheme more in line with the "S-to-S principle" is once-per-step adjustment of lateral foot placement; this has been analyzed by Townsend (1985). Turning, at least at low rates, can be done by the same mechanism.

Much of this discussion and development strategy can also apply to running. Running is of practical interest because walking has a fundamental speed limit of order $\sqrt{gl}$; at higher speeds centrifugal effect would lift the stance leg off the ground. It turns out that by adding a torsional spring at the hip and translational springs in each leg, the model of Figure 2 becomes a passive runner, with the same features of simplicity, efficiency, and ease of control that make passive walking attractive. Passive running has been described by McGeer (1989), and Thompson and Raibert (1989) have independently found similar behavior with both monoped and biped models. Investigation thus far has been limited to shallow slopes; as in walking, we have yet to do the steep-terrain and 3D investigations.

We hope that passive models will provide much insight into the dynamics and control of legged machines, but ultimately we must admit that this is only the easy part of the design problem. Legged locomotion is not competitive on smooth terrain; therefore practical machines must be capable of finding footholds and planning paths through difficult surroundings. Yet contemporary robots are hard pressed even to pick their way along paved highways and across flat floors! Thus it appears that the demands of a legged automaton must stimulate research for some years to come.

*Fig. 17. Notation for an
N-link, two-dimensional
open chain with rolling sup-
port.*

N–LINK 2–D CHAIN
WITH ROLLING SUPPORT
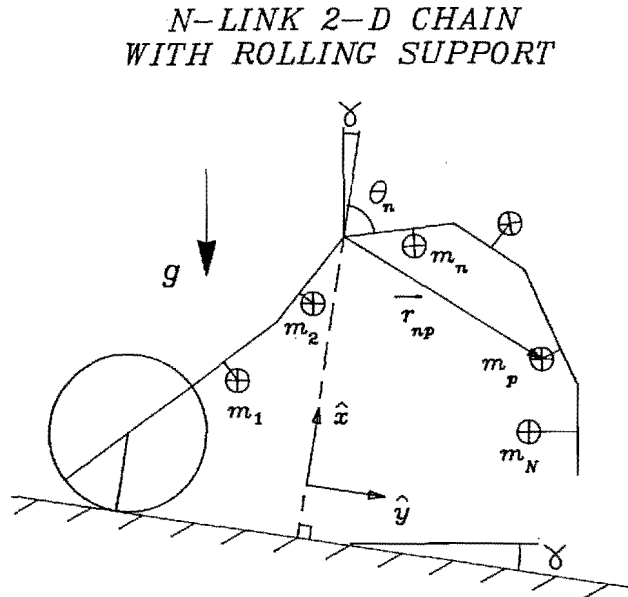
Appendix A. Dynamics of an N-Link Chain

Although we are interested in a machine with only
two rigid links, there is little extra effort involved in
generalizing to N links, and the more general result is
needed for a knee-jointed machine like that in Figure
16. The dynamics can be expressed in N second-order
equations of the form

$$\dot{H}_n = T_n, \tag{45}$$

where H_n is the angular momentum and T_n the torque
about the nth joint. In the case of $n = 1$, the "joint" is
the instantaneous point of contact. Simplification will
be afforded by subtracting equations for successive
joints, so that (45) becomes

$$\dot{H}_n - \dot{H}_{n+1} = T_n - T_{n+1}. \tag{46}$$

The torque is produced by gravity, and amounts to

$$T_{g_n} = \sum_{p=n}^{N} m_p \bar{r}_{np} \times \bar{g}; \tag{47}$$

Figures 17 and 18 provide the necessary notation. Then

$$T_{g_n} - T_{g_{n+1}} = \left(m_n \bar{r}_{nn} + \sum_{p=n+1}^{N} m_p \bar{l}'_n \right) \times \bar{g} \tag{48}$$

where $\bar{r}_{nn}$ is the vector from joint n to the mass center
of link n, and $\bar{l}'_n$ the vector from joint n to joint $n + 1$.
For link 1

$$\bar{r}_{11} = (c_1 - R)\hat{x}_1 + w_1\hat{y}_1 + R\hat{x}, \tag{49}$$

$$\bar{l}'_1 = (l_1 - R)\hat{x}_1 + R\hat{x}. \tag{50}$$

$\hat{x}_1$ and $\hat{y}_1$ are unit vectors fixed in link 1, as illustrated
by Figure 18.

For walking analysis we linearize the torque for
small $\Delta\theta$, γ. Thus from (18) and (19) we have

$$T_g = \begin{bmatrix} T_{g_1} - T_{g_2} \\ T_{g_2} - T_{g_3} \\ \vdots \\ T_{gN} \end{bmatrix} = K[\Delta\theta_W + b\gamma - \Delta\theta], \tag{51}$$

where $(K\Delta\theta_W)_n$ is the value of (48) at $\Delta\theta = 0$, $\gamma = 0$;
$(Kb)_n$ is the derivative of (48) with respect to γ, evalu-
ated at $\Delta\theta = 0$, $\gamma = 0$; and K_{nm} is the derivative of (48)
with respect to θ_m, evaluated at $\Delta\theta = 0$, $\gamma = 0$. For a
two-link chain with a point hip mass m_H, the results
are as follows:

$$K\Delta\theta_W = g \begin{bmatrix} m_1 w_1 \\ -m_2 w_2 \end{bmatrix} \tag{52}$$

$$Kb = g \begin{bmatrix} m_1 c_1 + (m_2 + m_H)l_1 \\ -m_2 c_2 \end{bmatrix} \tag{53}$$

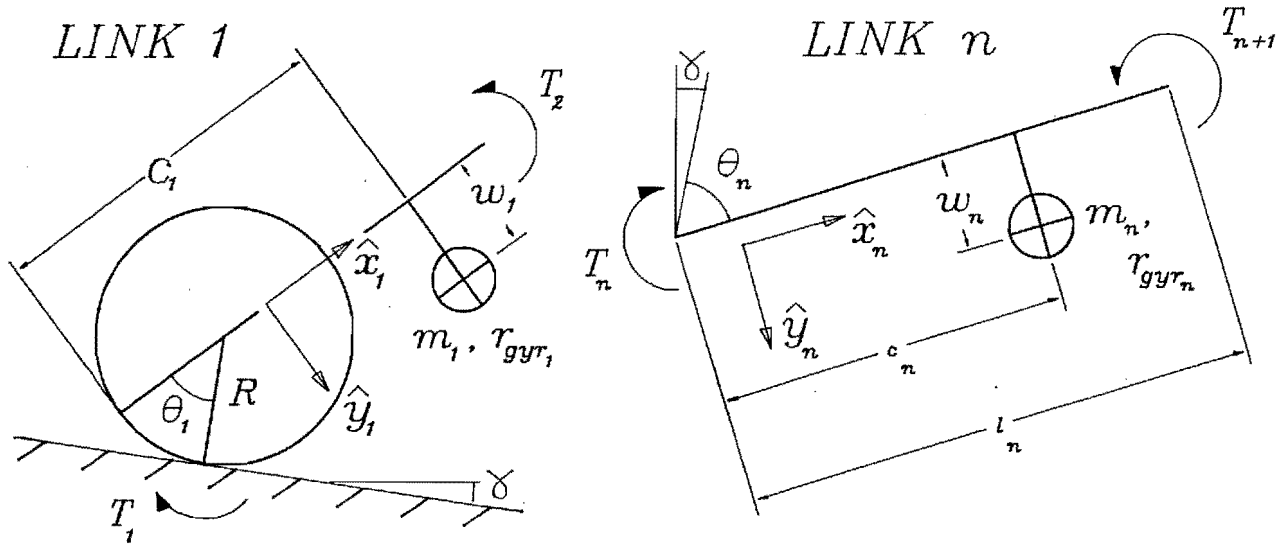$$K = -g \begin{bmatrix} m_1(c_1 - R) + (m_2 + m_H)(l_1 - R) & 0 \\ 0 & -m_2 c_2 \end{bmatrix} \tag{54}$$

Note that according to the convention of Figure 17, a
biped with matched legs has

$$m_2 = m_1, \tag{55}$$

$$c_2 = l_1 - c_1, \tag{56}$$

$$w_2 = -w_1. \tag{57}$$

Fig. 18. Notation for individual links of the chain.

LINK 1

LINK n

Now to work on the angular momentum terms in the equations of motion (46). H_n is

$$H_n = \sum_{p=n}^{N} m_p r_{gyr_p}^2 \Omega_p + \sum_{p=n}^{N} m_p \bar{r}_{np} \times \bar{V}_p. \quad (58)$$

Therefore

$$H_n - H_{n+1} = m_n r_{gyr_n}^2 \Omega_n + m_n \bar{r}_{nn} \times \bar{V}_n$$
$$+ \sum_{p=n+1}^{N} m_p \bar{l}_n' \times \bar{V}_p. \quad (59)$$

Equation (58) should be recognized as the angular momentum about a *stationary* point that is instantaneously coincident with joint n. Therefore, for the equations of motion (46) only Ω_n and $\bar{V}_n$ are differentiated:

$$\dot{H}_n - \dot{H}_{n+1} = m_n r_{gyr_n}^2 \dot{\Omega}_n + m_n \bar{r}_{nn} \times \dot{\bar{V}}_n$$
$$+ \sum_{p=n+1}^{N} m_p \bar{l}_n' \times \dot{\bar{V}}_p. \quad (60)$$

The kinematics of the chain are such that

$$\bar{V}_n = \Omega_n \times \bar{r}_{nn} + \sum_{p=1}^{n-1} \Omega_p \times \bar{l}_p', \quad (61)$$

where the Ω_n vector is directed into the page of Figure 17. This is differentiated for (60) as follows:

$$\dot{\bar{V}}_n = \dot{\Omega}_n \times \bar{r}_{nn} - \bar{r}_{nn}\Omega_n^2 + \sum_{p=1}^{n-1} \dot{\Omega}_p \times \bar{l}_p'$$
$$- \sum_{p=1}^{n-1} \bar{l}_p' \Omega_p^2 + R\Omega_1^2 \hat{x}. \quad (62)$$

The last term comes from differentiating $\bar{r}_{11}$ (49), and accounts for rolling of the contact point. Substituting into (60) leaves (after substantial but straightforward simplification)

$$\dot{H}_n - \dot{H}_{n+1} = \sum_{p=1}^{n-1} \bar{l}_p' \cdot \left(m_n \bar{r}_{nn} + \sum_{k=n+1}^{N} m_k \bar{l}_n' \right) \dot{\Omega}_p$$
$$+ \left(m_n r_{gyr_n}^2 + m_n |\bar{r}_{nn}|^2 + \sum_{k=n+1}^{N} m_k |\bar{l}_n'|^2 \right) \dot{\Omega}_n$$
$$+ \bar{l}_n' \cdot \sum_{p=n+1}^{N} \left(m_p \bar{r}_{pp} + \sum_{k=p+1}^{N} m_k \bar{l}_p' \right) \dot{\Omega}_p$$
$$+ \sum_{p=1}^{n-1} \bar{l}_p' \times \left(m_n \bar{r}_{nn} + \sum_{k=n+1}^{N} m_k \bar{l}_n' \right) \Omega_p^2$$
$$- \bar{l}_n' \times \sum_{p=n+1}^{N} \left(m_p \bar{r}_{pp} + \sum_{k=p+1}^{N} m_k \bar{l}_p' \right) \Omega_p^2$$
$$- R\hat{y} \cdot \left(m_n \bar{r}_{nn} + \sum_{k=n+1}^{N} m_k \bar{l}_n' \right) \Omega_1^2. \quad (63)$$

In matrix terms, as in (17), this can be expressed as

$$\dot{\mathbf{H}} = \begin{bmatrix} \dot{H}_1 - \dot{H}_2 \\ \dot{H}_2 - \dot{H}_3 \\ \vdots \\ \dot{H}_N \end{bmatrix} = \mathbf{M}\dot{\boldsymbol{\Omega}} + \mathbf{C}\boldsymbol{\Omega}^2. \qquad (64)$$

In stiff-legged walking the rotational speeds are small, so the Ω^2 term (centrifugal effect) can be neglected. (This approximation, however, is *not* valid for knee-jointed walking as in Figure 16). M is the inertia matrix; for a two-link biped

$$\mathbf{M} = \begin{bmatrix} m_1(r_{gyr_1}^2 + |\bar{r}_{11}|^2) + (m_2 + m_H)|\bar{l}_1'|^2 & m_2\,\bar{l}_1' \cdot \bar{r}_{22} \\ m_2\bar{l}_1' \cdot \bar{r}_{22} & m_2(r_{gyr_2}^2 + |\bar{r}_{22}|^2) \end{bmatrix}. \qquad (65)$$

In equation of motion (17), M is linearized; thus $\mathbf{M}_0$ is found by evaluating (65) with $\Delta\theta = 0$. However, for support transfer $\mathbf{M}^+$ (24) is evaluated with $\Delta\theta = \lambda\alpha$ (22).

Support transfer also involves the pre-transfer inertia matrix $\mathbf{M}^-$, which is calculated as follows. Equation (59) still holds for the angular momentum, but (61) is no longer correct for the velocity, since prior to transfer the chain is rolling about link N rather than link 1. Thus recasting (61) gives

$$\bar{V}_n^- = \Omega_n^- \times (\bar{r}_{nn} - \bar{l}_n') + \sum_{p=n+1}^{N} \bar{l}_p' \times \Omega_p^- + R(\hat{y} + \hat{y}_N)\Omega_N^-. \qquad (66)$$

Inserting this into (59) and collecting terms leaves

$$H_n - H_{n+1} = m_n(r_{gyr_n}^2 + |\bar{r}_{nn}|^2 - \bar{l}_n' \cdot \bar{r}_{nn})\Omega_n^- \\ - \sum_{p=n+1}^{N} \left(\left[m_n\bar{r}_{nn} + \sum_{k=n+1}^{p} m_k\bar{l}_n' \right] \cdot \bar{l}_p' - m_p\bar{l}_n' \cdot \bar{r}_{pp} \right)\Omega_p^- \\ + R\left(m_n\bar{r}_{nn} + \sum_{p=n+1}^{N} m_p\bar{l}_n' \right) \cdot (\hat{x} + \hat{x}_N)\Omega_N^-. \qquad (67)$$

For our machine, in matrix form, this is

$$\mathbf{M}^- = \begin{bmatrix} m_1(r_{gyr_1}^2 - \bar{r}_{11}) & (m_1\bar{r}_{11} + (m_2 + m_H)\bar{l}_1') \\ \cdot(\bar{l}_1' - \bar{r}_{11})) & \cdot(R(\hat{x} + \hat{x}_2) - \bar{l}_2) + m_2\bar{r}_{22} \cdot \bar{l}_1' \\ 0 & m_2(r_{gyr_2}^2 - \bar{r}_{22} \\ & \cdot(\bar{l}_2 - \bar{r}_{22}) + R\bar{r}_{22} \cdot (\hat{x} + \hat{x}_2)) \end{bmatrix}. \qquad (68)$$

Appendix B. Step-to-Step Transition Matrix

The S-to-S transition (36) has been derived by McGeer (1988); here we present only the final formula.

$$\mathbf{S} = \mathbf{S}_1^{-1}\mathbf{S}_2 \qquad (69)$$

where

$$\mathbf{S}_1 = \left[\begin{array}{c|cc|c} & 0 & 0 & -\frac{\partial \mathbf{D}_{\theta\theta}}{\partial\tau}[\lambda\alpha_0 \\ -\lambda & & & \\ & 0 & 0 & -\Delta\theta_{SE}] - \frac{\partial \mathbf{D}_{\theta\Omega}}{\partial\tau}\Omega_0 \\ \hline -\frac{\partial\Lambda}{\partial\alpha}(\mathbf{D}_{\Omega\theta}[\lambda\alpha_0 & 1 & 0 & -\Lambda\left(\frac{\partial \mathbf{D}_{\Omega\theta}}{\partial\tau}[\lambda\alpha_0 \right. \\ -\Delta\theta_{SE}] + \mathbf{D}_{\Omega\Omega}\Omega_0) & 0 & 1 & \left. -\Delta\theta_{SE}] + \frac{\partial \mathbf{D}_{\Omega\Omega}}{\partial\tau}\Omega_0 \right) \end{array} \right], \qquad (70)$$

$$\mathbf{S}_2 = \begin{bmatrix} \mathbf{D}_{\theta\theta}\lambda & \mathbf{D}_{\theta\Omega} \\ \Lambda\mathbf{D}_{\Omega\theta}\lambda & \Lambda\mathbf{D}_{\Omega\Omega} \end{bmatrix}. \qquad (71)$$

With the torque given by (18), the time derivative of D is

$$\frac{\partial \mathbf{D}}{\partial\tau} = \begin{bmatrix} \mathbf{D}_{\Omega\theta}^- & \mathbf{D}_{\Omega\Omega} \\ -\mathbf{M}_0^{-1}\mathbf{K}\mathbf{D}_{\Omega\theta} & -\mathbf{M}_0^{-1}\mathbf{K}\mathbf{D}_{\Omega\Omega} \end{bmatrix}. \qquad (72)$$

Appendix C. Explanation of Symbols

Roman

b	derivative of static equilibrium *w.r.t.* slope (19), (53)
c	Figs. 2, 18
D	start- to end-of-step transition matrix (20)
$D_{\theta\theta}$, $D_{\theta\Omega}$, $D_{\Omega\theta}$, $D_{\Omega\Omega}$	submatrices of start- to end-of-step transition matrix (27), (28)
D'	(32)
F	index exchanger (25)
$\bar{g}$	gravitational acceleration, Fig. 2
H	angular momentum
I	2×2 identity matrix
K	stance stiffness matrix (54)
l	leg length, Figs. 2, 18
$\bar{l}$	joint-to-joint vector (50), Fig. 18
M	inertia matrix (65), (68)
M_0	M for $\Delta\theta = 0$ (17), (65)
m	mass, Figs. 2, 17
m_H	hip mass fraction
R	foot radius, Fig. 2
$\bar{r}$	joint-to-mass center vector (49), Fig. 17
r_{gyr}	radius of gyration
S	step-to-step transition matrix (36), (69)
T	torque
V	linear velocity
w	offset from leg axis to leg mass center (Fig. 2)
$\hat{x}, \hat{y}$	unit vectors, Figs. 17, 18
z	eigenvalue of step-to-step equations (36)

Greek

α	leg angle at support transfer (22), Figs. 4, 5
γ	slope, Fig. 2
$\Delta\theta$	angle from surface normal, Fig. 2
η	coefficient of restitution (5)
$\Delta\theta_{SE}$	static equilibrium position (19)
$\Delta\theta_W$	static equilibrium on level ground (52)
Λ	support transfer matrix (26)
λ	support transfer vector (21)
σ	pendulum frequency (4)
τ	dimensionless time $t\sqrt{g/l}$
Ω	angular speed
ω_F	swing pendulum frequency
ω_R	lateral rocking frequency

Sub- and superscripts

+	immediately after support transfer
−	immediately before support transfer
0	steady cycle conditions
C	stance leg
F	swing leg
g	gravitational effect
k	step index

References

Lee, T-T., and Liao, J-H. 1988 (Philadelphia). Trajectory planning and control of a 3-link biped robot. *Proc. 1988 IEEE Int. Conf. Robot. Automat.* New York: IEEE, pp. 820–823.

Margaria, R. 1976. *Biomechanics and Energetics of Muscular Exercise.* Oxford, U.K.: Clarendon Press.

McGeer, T. 1988. Stability and control of two-dimensional biped walking. Technical report CSS-IS TR 88-01. Simon Fraser University, Centre for Systems Science, Burnaby, B.C.

McGeer, T. 1989. Passive bipedal running. Technical report CSS-IS TR 89-02. Simon Fraser University, Centre for Systems Science, Burnaby, B.C.

McMahon, T. 1984. Mechanics of locomotion. *Int. J. Robot. Res.* 3(2):4–28.

Mita, T., Yamaguchi, T., Kashiwase, T., and Kawase, T. 1984. Realisation of a high speed biped using modern control theory. *Int. J. Control* 40(1):107–119.

Miura, H., and Shimoyama, I. 1984. Dynamic walking of a biped. *Int. J. Robot. Res.* 3(2):60–74.

Mochon, S., and McMahon, T. 1980. Ballistic walking: An improved model. *Math. Biosci.* 52:241–260.

Raibert, M. 1986. *Legged Robots That Balance.* Cambridge, Mass.: MIT Press.

Russell, M. 1983. Odex 1: The first functionoid. *Robot. Age* 5:12–18.

Takanishi, A., Ishida, M., Yamazaki, Y., and Kato, I. The realisation of dynamic walking by the biped walking robot WL-10RD. *Proc. Int. Conf. Adv. Robot.* Tokyo: Robotics Society of Japan, pp. 459–466.

Thompson, C. and Raibert, M. (in press). Passive dynamic running. In Hayward, V., and Khatib, O. (eds.): *Int. Symposium of Experimental Robotics*. New York: Springer-Verlag.

Townsend, M. 1985. Biped gait stabilisation via foot placement. *J. Biomech.* 18(1):21–38.

Waldron, K., Vohnout, V., Perry, A., and McGhee, R. 1984. Configuration design of the adaptive suspension vehicle. *Int. J. Robot. Res.* 3(2):37–48.

Waldron, K. 1986. Force and motion management in legged locomotion. *IEEE J. Robot. Automat.* 2(4):214–220.

Yamada, M., Furusho, J., and Sano, A. 1985. Dynamic control of a walking robot with kick action. *Proc. Int. Conf. Adv. Robot.* Tokyo: Robotics Society of Japan, pp. 405–412.

Zheng, Y-F., Shen, J., and Sias, F. 1988 (Philadelphia). A motion control scheme for a biped robot to climb sloping surfaces. *Proc. 1988 IEEE Int. Conf. Robot. Automat.* New York: IEEE, pp. 814–816.